

Cite this: *RSC Sustainability*, 2023, 1, 282

# Kinetic and thermodynamic studies of HMF-ester synthesis using Brønsted–Lewis acidic ionic liquid catalyst†

Komal Kumar,<sup>a</sup> Shailesh Pathak,<sup>b</sup> Amit Kumar Rajora,<sup>c</sup> Anthony Halog<sup>\*,a</sup> and Sreedevi Upadhyayula<sup>\*,b</sup>

The valorization of 2nd generation biomass-derived 5-HMF into HMF-ester following the esterification reaction is a promising and appealing route for the production of renewable platform chemicals. Herein, we report the thermodynamics and kinetics of the HMF-ester products synthesized using bifunctional IL [SMIM][FeCl<sub>4</sub>] catalyst. The effects of the various reaction parameters such as reaction temperature and time were studied and optimized for maximum 5-HMF conversion into HMF-levulinate in a batch autoclave. Bifunctional IL [SMIM][FeCl<sub>4</sub>] catalyst gave 97% 5-HMF conversion with a maximum 78% yield of HMF-levulinate within 5 h reaction time at 378 K. The thermodynamic properties such as critical temperature ( $T_c$ ), critical volume  $V_c$ , critical pressure ( $P_c$ ), Gibbs free energy of formation ( $\Delta G_f^\circ$ ), enthalpy of formation ( $\Delta H_f^\circ$ ), and heat capacity ( $C_p$ ) for the HMF-ester products (HMF-levulinate, HMF-propionate, HMF-lactate, HMF-formate, and HMF-acetate) were estimated following the group contribution methods (GCMs). To elucidate the kinetics for the synthesis of HMF-levulinate, a series of the reaction runs were performed in a batch reactor in the temperature range of 348–393 K. Based on the results obtained by the experimental study, a reaction kinetic model for this HMF-levulinate synthesis reaction was formulated and the activation energy for the first order reaction was found to be 32.78 kJ mol<sup>-1</sup>.

Received 24th September 2022  
Accepted 17th December 2022

DOI: 10.1039/d2su00058j

rsc.li/rscsus

## Sustainability spotlight

HMF-esters are derived from platform chemical HMF and are obtained by lignocellulosic biomass valorization. They find potential applications as fungicides, fuel additives, surfactants, heat-activated crosslinkers for adhesives, coatings, composites, foundry binders, foams/inks, and also for treating sickle cell anemia. The scalability of such valuable HMF esters to industry scale production from the gram-scale laboratory synthesis needs the efficient design of suitable reactors, which is only feasible after establishing the thermodynamics and reaction kinetics, which is achieved in this work. Further, this work aligns with UN SDG 3 (good health and wellbeing), SDG 8 (decent work and economic growth), SDG 9 (industry, innovation, and infrastructure), and SDG 12 (responsible consumption and production).

## 1. Introduction

The valorization of 2nd generation lignocellulosic waste biomass materials into specialty chemicals, biofuel precursors, and fuel additives has gained extensive attention globally due to the ready availability and depletion of the fossil-based energy sources.<sup>1–3</sup> The production of biofuel and the

development of biorefineries is the best alternate tool for the transition from fossil-based resources to renewable energy sources.<sup>4</sup> Waste biomass (potentially green and renewable) is composed of lignin, hemicellulose, and cellulose, in which cellulose and hemicellulose contain 75% carbohydrates in polymer form, including both the six- and five-membered sugars.<sup>5–7</sup> Numerous industrially important products<sup>8</sup> and chemicals are being produced in biorefineries from biomass such as the industrial production of ethanol, lactic acid, 5-hydroxymethylfurfural (5-HMF), levulinic acid (LA), succinic acid, 2,5-furandicarboxylic acid, and sorbitol.<sup>4,9</sup> Different kinds of homogeneous and heterogeneous catalysts are reported for the conversion of lignocellulosic biomass into industrially important chemicals.<sup>10</sup> However, owing to the complex structure of biomass components involving inter- and intramolecular hydrogen bonding activation, the

<sup>a</sup>School of Earth and Environmental Sciences, The University of Queensland, Brisbane, Australia. E-mail: a.halog@uq.edu.au; Tel: +61 7 336 56141

<sup>b</sup>Department of Chemical Engineering, Indian Institute of Technology Delhi, Hauz Khas, New Delhi-110016, India. E-mail: sreedevi@chemical.iitd.ac.in; Fax: +91 11 26591120; Tel: +91 11 26591083

<sup>c</sup>Department of Chemistry, Indian Institute of Technology Delhi, Hauz Khas, New Delhi-110016, India

† Electronic supplementary information (ESI) available. See DOI: <https://doi.org/10.1039/d2su00058j>



conversion of these components into fine chemicals is still very difficult and challenging.<sup>11</sup> Researchers have reported the treatment of waste biomass in different kinds of acid and alkaline environments such as H<sub>2</sub>SO<sub>4</sub>, NaOH, and ammonia to break this inter and intramolecular hydrogen bonding but the conversion and recovery of the catalyst is still challenging.<sup>12</sup> In this context, ionic liquids (ILs) play an important role for biomass conversion into fine chemicals.<sup>11,13</sup>

Waste biomass-derived 5-hydroxymethylfurfural (5-HMF)<sup>14</sup> and levulinic acid (LA) have been identified as topmost specialty energy-rich chemicals.<sup>15,16</sup> The synthesis of these high value-added chemicals using environmentally-benign IL catalysts is reported in earlier literature.<sup>17–19</sup> The presence of highly reactive functional groups within 5-HMF and LA make both the chemicals important intermediate precursors for a host of different chemical reactions, such as esterification, acetalization, halogenation, hydrogenation, and condensation.<sup>20–24</sup> 5-HMF valorization is one of the thrust areas because of the wide application of its products, which include<sup>25,26</sup> resins, polymers, pharmaceuticals, antifreezing agents, fuels, and fuel additives. Among these, the upgraded HMF-ester products of 5-HMF following the esterification reaction are recognized as promising biofuel and fuel additive compounds.<sup>27,28</sup>

Esters are widely used in different industries such as food,<sup>29</sup> pharmaceutical,<sup>27</sup> and petroleum and petrochemicals.<sup>30,31</sup> Esters are usually synthesized by Fischer esterification, which is a classical acid-promoted organic reaction and predominantly catalyzed by mineral acid catalysts such as H<sub>2</sub>SO<sub>4</sub>, HF, and H<sub>3</sub>PO<sub>4</sub>.<sup>32</sup> The use of these mineral acid catalyst is advantageous due to full access to active sites and easy operation in homogeneous reaction conditions. However, mineral acid-catalyzed reactions have some disadvantages, including severe equipment corrosion, neutralization-generated gypsum waste, and problems in product purification, which has high energy consumption, high cost, and is environmentally hazardous. Hence, the synthesis of ester products using more efficient catalysts and green and sustainable process routes is highly demanding and desirable. Recently, the use of IL catalysts has increasingly become a more interesting approach<sup>33–36</sup> due to its advantageous properties such as high thermal stability, negligible volatility, selective solubility, and adjustable structural properties.<sup>37</sup> The reports on esterification reactions<sup>38,39</sup> are sparse; in addition, this reaction of 5-HMF with LA requires further investigation with regards to kinetic and thermodynamic aspects especially.

The thermodynamic physical properties such as liquid vapor pressure and normal boiling point of a compound are indispensable for the development of new processes and the optimization of the existing processes.<sup>40–43</sup> For instance, the accurate value of the liquid vapor pressure is required for many tasks in process simulation as well as for the determination of the number of theoretical stages in distillation columns and the calculation of temperature profiles. Similarly, the value of vapor pressure and normal boiling point express the stability and volatility of the fuel and have great importance for safety and environment concern<sup>42,43</sup> and required as entry data for the calculation of density, viscosity, surface tension, thermal

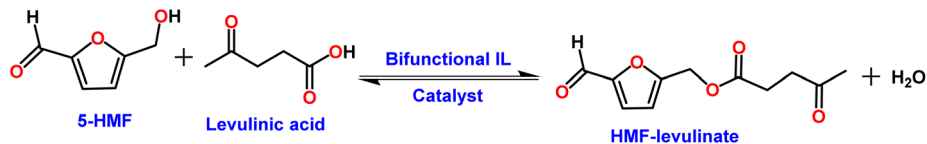
conductivity, enthalpy of vaporization, critical properties, and acentric factor.<sup>41,44,45</sup> On the other hand, critical properties such as critical temperature ( $T_c$ ) and critical pressure ( $P_c$ ) of the pure substance (compound) are commonly used in design and operation of the cyclic system.<sup>41,46</sup> However, the estimation of the experimental thermodynamic properties of the ester products has been a long-standing goal at the lab scale.<sup>47</sup> However, the determination of the thermodynamic properties of the biodiesel or biodiesel/biodiesel blends is impractical and difficult.<sup>40</sup> Therefore, thermodynamic models based on the correlations,<sup>48</sup> group contribution techniques,<sup>49–52</sup> and the method based on the principle of corresponding states are very helpful to estimate these properties with more accurate results.<sup>53</sup> Among all these, the GCMs are the most successful predictive methods and can be selected as promising for the estimation of the thermodynamic properties, which were developed in 1950s.<sup>54</sup>

According to the group contribution approach, the property of a molecule is a function of the structurally-dependent parameter and can be determined by summing the frequency of each group occurring in the molecule times its contribution.<sup>46</sup> In addition, the behavior of a substance is strongly dependent over the intermolecular forces and the types of the chemical bonds within the molecule. Following GCMs, thermodynamic properties such as  $T_c$ ,  $P_c$ , normal boiling point ( $T_b$ ),<sup>49,50,55–59</sup> enthalpies of formation, entropies,<sup>60</sup> and activity coefficients can be estimated.<sup>54</sup> In previous studies, following this approach, Z. Kolska estimated the enthalpy and entropy of vaporization of organic compounds.<sup>51</sup> R. Ceriani and coworkers estimated the vapor pressure and heats of vaporization of edible oil/fat compounds.<sup>61</sup> B. Moller *et al.* estimated the vapor pressure of non-electrolyte organic compounds.<sup>62</sup> Sales-Cruz and coworkers estimated  $T_c$  and  $P_c$  for fatty acid alkyl esters compounds.<sup>63</sup> Wallek *et al.* recently reported the  $T_c$ ,  $P_c$ , and  $T_b$  of the compounds.<sup>64</sup> Similarly, the thermodynamic physical properties of the fatty acid esters and multifunctional organic compounds was estimated by Wang *et al.* and J. F. Pankow *et al.*, respectively.<sup>65,66</sup>

On the other hand, a number of the kinetic studies have appeared on the synthesis of the esters, which help us to ascertain the boundaries of feasibility of the reaction investigations and are important to assess the activation energy of the esterification reaction.<sup>67</sup> In the earlier reported studies, the kinetics of the esterification reactions have been reported by different research groups.<sup>68–70</sup> However, to the best of our knowledge, the thermodynamic properties for various organic compounds and kinetics for different esterification reactions have been reported in the previous studies, whereas the available data does not cover the thermodynamics of HMF-ester products, which are derived by the reaction of 5-HMF with acid components. In addition, the kinetics for the 5-HMF esterification reaction is still missing in the literature. The esterification reaction scheme of the HMF-levulinate with the esterification reaction of 5-HMF and LA is represented in Scheme 1.

The objective of the present study is to develop the reaction kinetics for the esterification of HMF into HMF-levulinate using Brønsted–Lewis (bifunctional) acidic IL [SMIM][FeCl<sub>4</sub>] catalyst.





Scheme 1 Esterification reaction scheme of 5-HMF with LA.

To perform the kinetic study of this reaction, the effect of the reaction kinetic parameters such as time and temperature on the 5-HMF conversion was studied. From the kinetics, the reaction rate constant, activation energy ( $E_a$ ), and pre-exponential factor ( $A$ ) were estimated. Similarly, HMF-formate, HMF-lactate, HMF-propionate, and HMF-acetate were synthesized with the reaction of 5-HMF with formic acid, lactic acid, propionic acid, and acetic acid. Our current study is also focussed on predicting the thermodynamic properties of HMF-ester compounds, such as critical temperature, critical pressure, and critical volume based on GCMs. This study also estimates the thermodynamic properties of HMF-ester compounds such as Gibbs free energy ( $\Delta G_f^0$ ), enthalpy ( $\Delta H_f^0$ ), and heat capacity ( $C_p$ ) using the GCMs.

## 2. Materials and methods

### 2.1 Materials

HMF (97%), 1-methyl imidazole (99%), LA (99%), and propionic acid (99%) were purchased from Alfa Aesar, China. Lactic acid (LAC) (88%), formic acid (FA) (99%), and acetic acid (85%) were purchased from Fischer Scientific India. Chlorosulfonic acid (98%) was purchased from Spectrochem India Pvt. Ltd. Diethyl ether, *n*-hexane, anhydrous  $\text{FeCl}_3$  (97%), ethyl acetate, and 4 Å molecular sieves were purchased from Merck, India. All the other required chemicals from commercial sources used were at high purity level. The solvents were dried with 4 Å molecular sieves by gently shaking overnight prior to use. 4 Å molecular sieves (MS) were dried overnight at 408 K prior to use.

### 2.2 Synthesis of the Brønsted–Lewis (bifunctional) acidic IL catalysts ([SMIM][FeCl<sub>4</sub>])

The bifunctionalized IL catalyst, [SMIM][FeCl<sub>4</sub>], was synthesized as per the previously reported synthetic procedure.<sup>71</sup> For the synthesis of the bifunctional IL catalyst [SMIM][FeCl<sub>4</sub>], first Brønsted acidic IL [SMIM][Cl] was synthesized following the

decanted. The unreacted species were removed by washing the resultant mixture with  $\text{CH}_2\text{Cl}_2$ , dried using a rotary evaporator, and the product was dried at 353 K. The synthesized Brønsted acidic IL [SMIM][Cl] was characterized following the <sup>1</sup>H NMR and <sup>13</sup>C NMR spectroscopic techniques. Finally, [SMIM][FeCl<sub>4</sub>] was synthesized by mixing equimolar amounts of anhydrous  $\text{FeCl}_3$  within [SMIM][Cl] at room temperature, followed by vigorous stirring, and characterized as reported in the literature.<sup>23</sup>

### 2.3 Catalytic activity for 5-HMF conversion into HMF-esters

HMF-ester products were synthesized in a batch reactor; all experiments were conducted in a 25 mL round bottom (RB) flask and heated in an oil bath at the required optimum reaction temperature. The RB flask was connected with a reflux condenser and the inert atmosphere inside the reaction was created by adjusting the nitrogen balloon at the top of the reflux condenser. The reaction was conducted by adding 1.2 mmol 5-HMF and 6 mmol acid (LA, formic acid, lactic acid, propionic acid, and acetic acid) into the flask. The resultant reaction mixture was stirred magnetically under an inert atmosphere at room temperature. Further, 150 mg bifunctional IL catalyst and 150 mg 4 Å dried molecular sieves were added into the reaction mixture, and the reaction temperature was increased to the desired value to attain a certain reaction temperature, which was measured using a thermocouple within the oil bath. After the completion of the reaction, the sample was collected and the quantitative conversion of 5-HMF was analyzed by high pressure liquid chromatography (HPLC).

### 2.4 HPLC analysis

HPLC was used for detecting the conversion of 5-HMF into HMF-esters, and the separation and purification of the product were done according to the same procedure as described in our previous studies.<sup>23,72</sup> Finally, the conversion of 5-HMF was

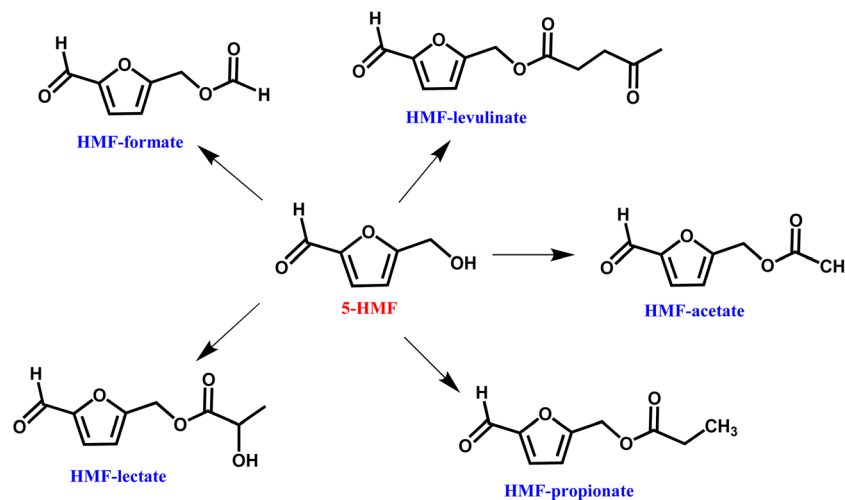
$$\text{5-HMF conversion(\%)} = \frac{\text{Initial moles of 5-HMF used} - \text{remaining no. of moles of 5-HMF after reaction}}{\text{Initial no. of moles of the 5-HMF added}} \times 100\% \quad (1)$$

earlier reported procedure. In a typical synthesis, chlorosulfonic acid ( $\text{SO}_3\text{HCl}$ ) was added dropwise at room temperature in a slight excess of 1-methylimidazole in dry dichloromethane ( $\text{CH}_2\text{Cl}_2$ ) solvent. The resultant reaction mixture was stirred for 20 minutes and after the completion of the reaction, solvent was

determined according to eqn (1)

The yield of the product was determined according to eqn (2).





Scheme 2 Synthesized HMF-ester products from 5-HMF and different acids.

$$\text{Yield (\%)} = \frac{\text{No. of moles of product obtained}}{\text{Initial no. of moles of 5-HMF used}} \times 100\% \quad (2)$$

The selectivity of the product was determined according to eqn (3)

$$\text{Selectivity(\%)} = \frac{\% \text{ Yield of obtained product}}{\% \text{ Conversion of 5-HMF}} \times 100\% \quad (3)$$

## 2.5 Estimation of thermodynamic property

The HMF-ester products (synthesized by the reaction of 5-HMF with different acids (formic acid, LA, propionic acid, acetic acid, and lactic acid)) are represented in Scheme 2. The HMF-ester products represented in Scheme 2 were successfully synthesized using a bifunctional IL catalyst developed in the lab and characterized previously.<sup>23</sup> To calculate the thermodynamic properties of the HMF-ester products, different GCMs were employed. All the estimated thermodynamic properties such as critical temperature, critical pressure, and critical volume, Gibbs free energy, and enthalpy of the formations are based on the GCMs. In the GCMs, the critical properties of a compound are considered to be the sum of the contribution values of all, *i.e.*, based on the contribution of elements or functional groups, isomers, and chemical bonds. The GCMs, namely, Constantinou and GANI, JOBACK, AMBROSE, FEDORS, LYDERSEN, and BENSON, were employed to determine the thermodynamic properties of HMF-esters.

## 2.6 Methods used in the estimation of the thermodynamic properties

The thermodynamic parameters such as change in Gibbs free energy ( $\Delta G$ , J mol<sup>-1</sup>) and enthalpy change ( $\Delta H$ , J mol<sup>-1</sup>) were estimated using ASPEN PLUS. The properties of the ester products (shown in Scheme 2) were estimated using appropriate GCMs.<sup>73</sup> Thermodynamic physical property data  $T_c$  and

( $P_c$ ) for the HMF-esters were calculated using the best GCMs, which shows somewhat more accurate results with minimum error value compared to the other GCMs. A comparison of the deviations of the calculated thermodynamic property values for 5-HMF from the experimental and estimated values between the different group contribution methods is summarized in Table S1, ESI.† It gives the number of model parameters and average percent deviations of the thermodynamic property estimation for the GCMs. When the thermodynamic critical property value was estimated using the JOBACK and GANI GCMs, the estimated error value was relatively lower with more accurate predictions as compared with LYDERSEN, BENSON, and FEDORS GCMs. Henceforth, JOBACK method was implemented to estimate ( $P_c$ ) and ( $T_c$ ) values for the HMF-ester compounds. On the other hand, GANI GCM used to estimate the normal boiling point ( $T_b$ ),  $\Delta H_f^0$ , and  $\Delta G_f^0$ . The GANI method is a combination of two levels of approximation wherein the basic level only used the contribution from the first-order groups while the second level considers the effects among groups and isomers and gives more accurate results. Similarly, the value of heat capacity was calculated using JOBACK and BENSON GCMs. It is seen that the BENSON method showed somewhat more accurate predictions with relatively minimum error value compared with the JOBACK method. The equations used to estimate the thermodynamic properties of pure components are as follows.

The value of  $T_b$ , ideal gas heat capacity ( $C_p$ ), and standard Gibbs free energy ( $\Delta G_{f,298.15\text{ K}}^0$ ) were calculated using the JOBACK method.

$$T_b \text{ (K)} = -75.15 + \sum_i n_i t_{b,i} + 273.15 \quad (4)$$

Ideal gas heat capacity:

$$C_p \text{ (J mol}^{-1} \text{ K}^{-1}) = \sum a_i - 37.93 + [\sum b_i + 0.210]T + [\sum c_i - 3.91 \times 10^{-4}] + [\sum d_i + 2.06 \times 10^{-7}]T^3 \quad (5)$$



Standard Gibbs free energy:

$$\Delta G_{T_{25}^{\circ}\text{C}} \text{ (kJ mol}^{-1}\text{)} = 53.88 + \sum_i n_i g_{f,i} \quad (6)$$

$$K = \exp \left[ -\frac{\Delta_r G(T)}{RT} \right] \quad (16)$$

LYDERSEN method was employed for the estimation of  $T_c$  followed by the equation as given below.

$$T_c \text{ (K)} = \frac{T_b + 273.15}{0.567 + \sum_i t_{c,i} - \left( \sum_i t_{c,i} \right)^2} + 273.15 \quad (7)$$

The  $P_c$  value of the HMF-esters was estimated, followed by the AMBROSE method, and the used equation is as given below.

$$P_c \text{ (atm)} = \frac{M}{\left( 0.34 + \sum_i n_i P_{c,i} \right)^2} \quad (8)$$

The  $V_c$  value of the HMF-ester compounds was calculated using the FEDORS method with the following equation.

$$V_c \text{ (m}^3 \text{ kmol}^{-1}\text{)} = \frac{26.6 + \sum_i n_i v_{c,i}}{1000} \quad (9)$$

The BENSON method was also employed for the estimation of Gibbs free energy and enthalpy of formation.

The enthalpy of formation was calculated using the following equation.

$$\Delta H_{f,298.15}^0 = \sum_i n_i \Delta H_{f,298.15,i}^0 \quad (10)$$

Gibbs free energy was calculated using the given equation.

$$\Delta G_f^0 = \Delta H_{f,298.15}^0 - 298.15 \Delta S_{f,298.15}^0 \quad (11)$$

Specific heat capacity was calculated using the following equation.

$$C_p^0(T) = \sum_k N_k C_{pk}^0(T) \quad (12)$$

where  $M$  is the molar mass,  $n_i$  is the total number of the groups of type- $i$  in the compound,  $t_{c,i}$ ,  $p_{c,i}$ ,  $t_{b,i}$ ,  $v_{c,i}$ ,  $h_{f,i}$  and  $g_{f,i}$  are the contribution values for each group of type- $i$  for the estimation of  $T_c$ ,  $P_c$ ,  $T_b$ ,  $V_c$ ,  $\Delta H_f^0$ , and  $\Delta G_f^0$ , respectively, and  $N$  is the number of atoms in the molecule.

The GANI method was used for the calculation of the following values.

Standard value of vaporization of enthalpy and entropy:

$$\Delta H_f^0(l) = \Delta H_f^0(g) - \Delta H_v^0 \quad (13)$$

$$S_{298.15}^0(l) = S_{298.15}^0(g) - S_v^0 \quad (14)$$

Calculation of Gibbs free energy and equilibrium constant:

$$\Delta_r G_{298.15}^0 = \Delta_r H_{298.15}^0 - T \Delta_r S_{298.15}^0 \quad (15)$$

## 2.7 Kinetics of the esterification reaction of 5-HMF with LA

In the kinetic study, all the experiments for the esterification of 5-HMF with LA were conducted in a batch reactor (25 mL round bottom flask) with 5-HMF as the limiting reactant and LA as the excess reactant to get the maximum conversion of 5-HMF into the desired product in the temperature range of 348–393 K. Based on the experimental data, a reaction kinetic model was developed.

## 3. Results and discussion

### 3.1 Characterization of the synthesized Brønsted acidic IL [SMIM][Cl]

The  $^1\text{H}$  and  $^{13}\text{C}$  NMR data of [SMIM][Cl] are as follows:  $^1\text{H}$  NMR (400 MHz, DMSO- $d_6$ ):  $\delta$  (ppm) 3.85 (s, 3H), 7.67 (t, 1H), 9.06 (t, 1H), 12.20 (s, 1H), and 14.51 (s, 1H).  $^{13}\text{C}$  NMR: (100 MHz;  $\text{D}_2\text{O}$ ):  $\delta$  (ppm) 36.45, 122.02, 123.4, and 137.6.

### 3.2 Determination of the acidity of the bifunctional [SMIM][FeCl<sub>4</sub>] IL catalyst

The acidity of the bifunctional IL [SMIM][FeCl<sub>4</sub>] catalyst was determined using an acid–base titration method according to the procedure reported earlier.<sup>36</sup> The desired amount of the bifunctional IL was dissolved in 2-propanol and the mixture was then titrated with 0.1 M NaOH with phenolphthalein as the indicator. When the colorless solution turns pink, it was considered as the end-point of the titration. A blank titration was also performed. Finally, the acid value was calculated, which is defined as the amount of NaOH required to neutralize 1 g bifunctional IL catalyst, using following the equation.

$$\text{Acid value (g/g)} = \frac{(A - B) \times M \times 40}{W}$$

where  $A$  is the volume of NaOH required for the titration of the sample (mL),  $B$  is the volume of NaOH required for the titration of the blank (mL),  $M$  is the molarity of the NaOH solution, and  $W$  is the sample mass (g). Finally, the acidity of the bifunctional IL, [SMIM][FeCl<sub>4</sub>] was found to be  $0.92 \pm 0.04$  g NaOH/g IL.

### 3.3 Conversion of 5-HMF into HMF-levulinate and the effect of the reaction time and temperature on 5-HMF conversion

The effect of the reaction time and temperature on the 5-HMF conversion and HMF-levulinate yield are represented in Fig. 1. Using the bifunctional [SMIM][FeCl<sub>4</sub>] IL catalyst, the effect of the reaction time and temperature on the 5-HMF conversion was investigated at 348–393 K up to 6 h reaction time. The conversion of 5-HMF into HMF-levulinate significantly increases with increasing reaction time and temperature. At 348 K, the conversion of 5-HMF into HMF-levulinate significantly increases and reaches 66% within 5 h reaction time, whereas as the reaction temperature increased from 348 K to



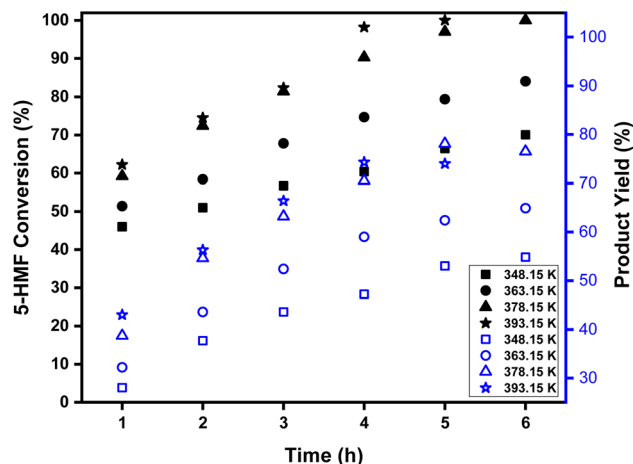


Fig. 1 Conversion of 5-HMF into HMF-levulinate with time and temperature. Reaction conditions: 5 : 1 molar ratio (LA : HMF), 150 mg catalyst, molecular sieves, 300 rpm.

363 K, 5-HMF conversion increased from 66% to 79% at 5 h reaction time. Similarly, at 378 K, the conversion of 5-HMF reached up to 97% within 5 h reaction time, and the maximum (78%) yield of HMF-levulinate was obtained. This result confirms that the reactivity of 5-HMF as well as the yield of HMF-levulinate increases till a reaction temperature of up to 378 K. On the contrary, as the reaction time increases at this temperature, the conversion of 5-HMF reached up to 100%, whereas the yield of HMF-levulinate decreased significantly because the longer reaction time increased the 5-HMF conversion into its byproduct humin. 98% 5-HMF conversion was obtained within 4 h as the reaction temperature was increased up to 393 K. However, the high reaction temperature had a negative effect on the HMF-levulinate yield and the product selective yield decreased and reached up to 74% at this time and temperature. At 393 K and 5 h reaction time, 100% conversion of 5-HMF was achieved, whereas no significant improvement in the HMF-levulinate yield was observed because high reaction temperature and long reaction time led to a high polymerization of 5-HMF into a black mass of humin byproduct. Finally, at 378 K and 5 h, the highest yield (78%) of HMF-levulinate and 97% 5-HMF conversion were achieved, making them the best optimized reaction conditions for 5-HMF esterification to HMF-levulinate.

### 3.4 Conversion of the different acids into the HMF-ester product

The esterification reaction of 5-HMF into HMF-ester products was conducted to investigate the possibility of extending the scope of 5-HMF into its different HMF-ester products. The laboratory-synthesized bifunctional IL was tested in the 5-HMF conversion to HMF-ester products such as HMF-formate, HMF-lactate, HMF-propionate, and HMF-acetate at the established optimum reaction conditions for the HMF-levulinate synthesis, except for the HMF-formate synthesis. The conversion of 5-HMF into different HMF-ester products and the product yields are

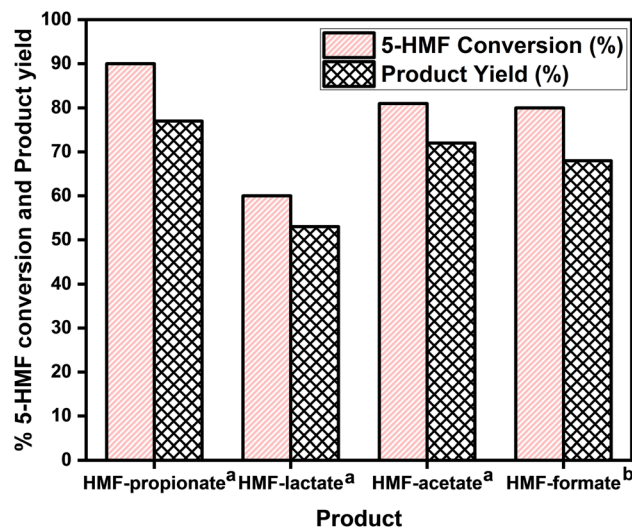


Fig. 2 Synthesis of different HMF-ester products. <sup>a</sup>Reaction conditions: 5 : 1 molar ratio of acid to 5-HMF, 150 mg catalyst, 150 mg molecular sieve,  $T = 378$  K,  $t = 5$  h, 300 rpm. <sup>b</sup>Reaction conditions: 5 : 1 molar ratio of acid and 5-HMF, 150 mg catalyst, 150 mg molecular sieve,  $T = 363$  K,  $t = 5$  h, 300 rpm.

shown in Fig. 2. The proposed reaction method was successfully employed for the conversion of 5-HMF into its ester products. Using the bifunctional [SMIM][FeCl<sub>4</sub>] IL catalyst, high conversion of 5-HMF was achieved with good yield of the HMF-ester products. As the esterification reaction of 5-HMF was conducted using propionic acid and [SMIM][FeCl<sub>4</sub>] IL catalyst at 378 K and 5 h reaction time, a maximum 90% 5-HMF conversion with 77% HMF-propionate was obtained. In the case of lactic acid, 60% 5-HMF conversion with 53% HMF-lactate yield was obtained at 378 K and 5 h. On the other hand, when the esterification reaction of 5-HMF was performed with acetic acid under similar reaction conditions, 81% 5-HMF conversion with 72% HMF-acetate was obtained. In the case of formic acid, the esterification reaction of 5-HMF was performed at 363 K, and 68% yield of the HMF-formate was obtained with 80% 5-HMF conversion. The difference in the 5-HMF conversion as well as in the product yield can be attributed to the different acidic strengths of the corresponding acids, which affect the overall acidity of the reaction medium and varied the product yield and 5-HMF conversion. However, good to moderate yield of the HMF-ester products was obtained using the bifunctional [SMIM][FeCl<sub>4</sub>] IL catalyst. These results confirm that the synthesis of different HMF-ester products is feasible using this bifunctional IL catalyst.

### 3.5 Kinetic study of HMF-levulinate synthesis

As shown in the reaction Scheme 1, the reaction kinetics of HMF-levulinate synthesis are presented in this section from the obtained experimental results with the esterification reaction of 5-HMF and LA using the bifunctional IL catalyst at different times and temperatures. Numerous reaction experiments were performed over different times and temperatures, as represented in Fig. 1, using 1 : 5 molar ratio of 5-HMF and LA in the



range of 348–393 K. The rate constant was calculated according to eqn (17). The experimental data obtained from the reaction at different temperatures and times were used to derive the kinetic model for this reaction.

Here, HMF-levulinate synthesis reaction kinetics was determined following the integral method and the rate of the reaction can be written as follows.

$$\frac{-dC_{5\text{-HMF}}}{dt} = k_1 C_{5\text{-HMF}}^a C_{\text{LA}}^b - k_2 C_{\text{HMF-levulinate}}^c C_{\text{W}}^d \quad (17)$$

where  $k_1$  is the rate constant for the forward reaction,  $k_2$  is the reaction rate constant of backward reaction, a, b, c, and d are the number of reaction order of 5-HMF, LA, HMF-levulinate, and water for forward and backward reaction, respectively (Scheme 1). Here, the LA is present in high concentration (5-HMF : LA (1 : 5)) compared with 5-HMF in the reaction; therefore, the possibility of backward reaction is considered as negligible and the reaction rate of the HMF-levulinate synthesis can be written as follows.

$$\frac{-dC_{5\text{-HMF}}}{dt} = k_1 C_{5\text{-HMF}}^a C_{\text{LA}}^b \quad (18)$$

As the concentration of LA is in excess amount,  $k_1 C_{\text{LA}}^b$  is constant and eqn (18) can be transformed into

$$r_{5\text{-HMF}} = k C_{5\text{-HMF}}^n \quad (19)$$

The esterification rate for 5-HMF with LA is defined as  $X$ , the initial concentration is  $C_{5\text{-HMF},0}$ , and the concentration of 5-HMF in the esterification reaction system at any time is  $C_{5\text{-HMF}}$ ; then,  $C_{5\text{-HMF}} = C_{5\text{-HMF},0}(1-X)$ .

$$r_{5\text{-HMF}} = \frac{-dC_{5\text{-HMF}}}{dt} = \frac{-d[C_{5\text{-HMF},0}(1-X)]}{dt} = k C_{5\text{-HMF}}^n \quad (20)$$

Then,

$$\frac{dX}{(1-X)^n} = \frac{k}{C_{5\text{-HMF},0}^{1-n}} dt \quad (21)$$

After integration on both sides, eqn (21) can be written as follows.

$$(1-X)^{1-n} = \frac{k(n-1)}{C_{5\text{-HMF},0}^{1-n}} t \quad (22)$$

Finally, at different reaction temperatures, a graph between the 5-HMF concentration and reaction time were obtained (Fig. 3 (a-c)) using eqn (22). The value of  $\ln(1-X)$  is linear with  $t$  at  $n = 1$ ,

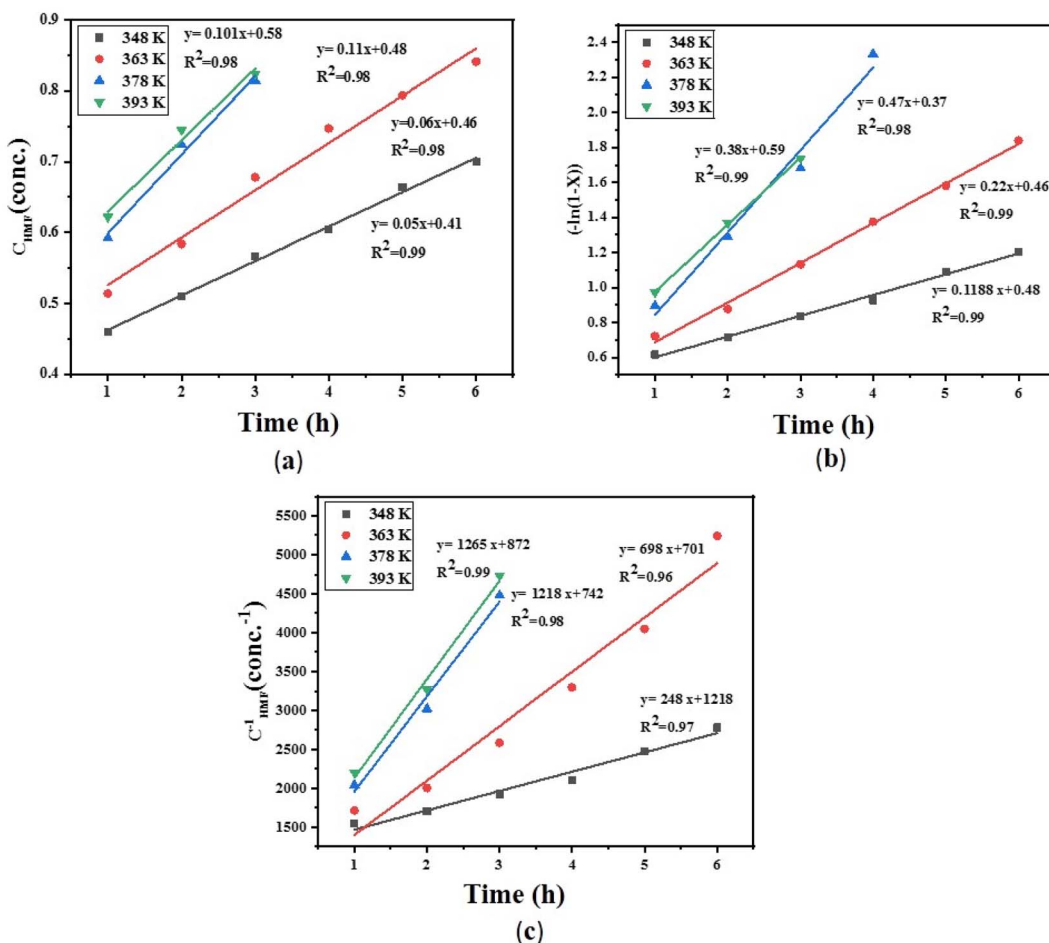


Fig. 3 (a) Conversion of 5-HMF at different reaction times for (a) zero order, (b) first order, (c) second order reaction.



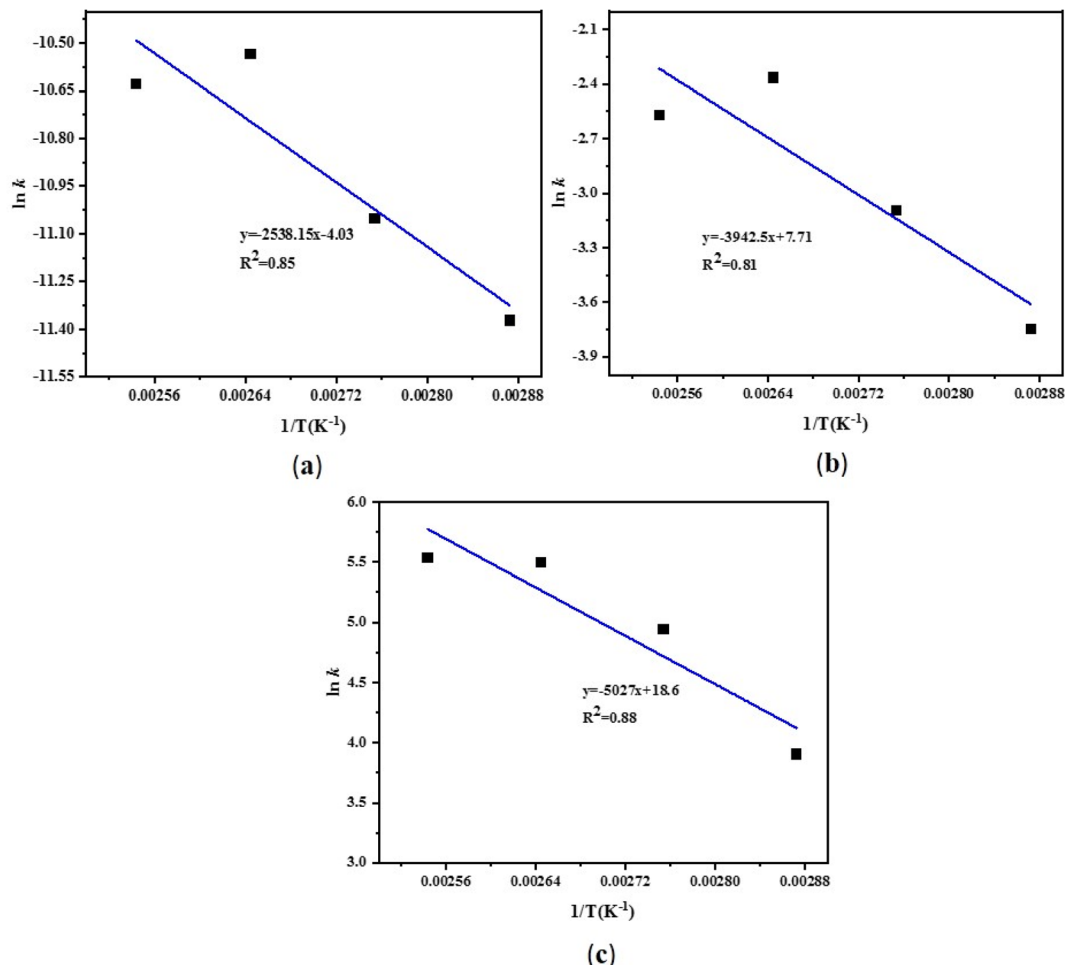


Fig. 4 Arrhenius plot for the esterification of 5-HMF with LA (a) zero order, (b) first order, and (c) second order reaction.

whereas at  $n \neq 1$ ,  $(1 - X)^{(1-n)}$  and time have a linear relationship. The Arrhenius plot for the HMF-levulinate synthesis is shown in Fig. 4(a-c), and the value of the correlation coefficient can be estimated for different values of  $n$ . Accordingly, the variation in the reaction rate with temperature may be expressed by the Arrhenius equation.

$$\ln k = \ln A - \frac{E_a}{RT} \quad (23)$$

where  $T$  indicates the reaction temperature and  $R$  is the gas constant. Thus, the value of  $E_a$  (activation energy) and  $k_0$  (pre-exponential factor) can be derived from the Arrhenius ( $\ln k$  vs.  $1/T$ ) plot. The calculated  $E_a$  for the different reaction orders are shown in Table 1. The activation energy was in the range of

21.10–41.80  $\text{kJ mol}^{-1}$ . For the first order reaction, the activation energy was 32.78  $\text{kJ mol}^{-1}$ . These results unambiguously provide strong evidence that the used bifunctional catalyst for the HMF-levulinate synthesis is an efficient and active catalyst.

### 3.6 Comparison of the kinetics of the previously reported esterification reactions

The comparison of the previously reported kinetics studies for the different reactants (acid and alcohols) is summarized in Table 2. In the earlier studies, several kinetic models are reported for the esterification reaction with the consideration of different types of assumptions. In 1994, H. J. Bart *et al.* reported the esterification reaction of LA with n-butanol using  $\text{H}_2\text{SO}_4$

Table 1 Reaction order, pre-exponential, and activation energy for the esterification reaction

Reaction order	Kinetics	Activation energy ( $\text{kJ mol}^{-1}$ )	Pre-exponential factor ( $(\text{min})^{-1}(\text{mol L}^{-1})^{1-n}$ )	$R^2$
0 order reaction	$C_{G0} - C_G = kt$	21.10	56.50	0.85
1st order reaction	$-\ln(1 - X) = kt$	32.78	$22.4 \times 10^2$	0.82
2nd order reaction	$\frac{1}{C_{5\text{-HMF}}} - \frac{1}{C_{5\text{-HMF},0}} = kt$	41.80	$11.50 \times 10^7$	0.88



mineral acid catalyst, and the activation energy for this study was 54.27 kJ mol<sup>-1</sup>.<sup>74</sup> In 1991, S. Goto and coworkers reported the esterification reaction of isobutyl alcohol with palmitic acid using sulfuric acid catalyst and reported 58.0 kJ mol<sup>-1</sup> activation energy.<sup>75</sup> R. Aafaqi *et al.* studied the esterification reaction of palmitic acid with isopropanol using *p*-TSA. This study reported 40.77 kJ mol<sup>-1</sup> activation energy for this reaction.<sup>76</sup> W. Shi and coworkers reported the esterification reaction of palmitic acid and isobutyl alcohol using a novel composite catalytic membrane (CCM) as a heterogeneous catalyst, which was prepared from sulfonated polyethersulfone (SPES) and polyethersulfone (PES) blend supported by non-woven fabrics. This study reported 35.97 kJ mol<sup>-1</sup> activation energy for this reported system.<sup>77</sup> S. H. Ali *et al.* reported the esterification (benzyl alcohol and acetic acid) and hydrolysis (benzyl acetate) process using Dowex 50 Wx8-catalyst with 54.5–57 kJ mol<sup>-1</sup> activation energy.<sup>69</sup> In 2019, L. J. Wei *et al.* reported the kinetics and esterification of acrylic acid and ethanol over the solid acid catalyst Amberlyst 35 and reported an activation energy of 59.60 kJ mol<sup>-1</sup>.<sup>68</sup> In 2020, S. Chaemchuen *et al.* reported the esterification of oleic acid into methyl oleate using UiO-66 MOF catalyst with an activation energy of 54.9 ± 1.8 kJ mol<sup>-1</sup>.<sup>70</sup> Novozyme 435 catalyzed enzymatic esterification of 5-HMF was reported by Y. Z. Qin group and lipase-catalyzed transesterification of 5-HMF esters was reported by M. Krystof and coworkers; however, their kinetic study has not been reported.<sup>27,78</sup> Among the reported kinetics for similar esterification reactions, the activation energies ranged from 35 to 60 kJ mol<sup>-1</sup> as shown in Table 2. In this study, bifunctional IL catalyst successfully catalyzed the esterification reaction and

the activation energy for this reaction was found in the range of 32.78 kJ mol<sup>-1</sup> for the first order reaction. Finally, the activation energy is lower than the earlier reported studies compared in Table 2. The obtained results show beneficial results for the esterification reaction of 5-HMF with LA.

### 3.7 Estimation of the thermodynamic parameters for HMF-ester products

The value of the critical properties such as  $T_c$ ,  $P_c$ , and  $V_c$  for the HMF-ester compounds (HMF-levulinate, HMF-acetate, HMF-propionate, HMF-lactate, and HMF-formate) were estimated, followed by using the most appropriate GCMs, which showed the lowest error values. The JOBACK method was employed to estimate the value of critical properties such as  $T_c$  and  $P_c$  for the HMF-ester compounds, and their estimated results are shown in Table 3. Similarly, the LYDERSEN method was employed to estimate the  $V_c$  value. The esters derived from 5-HMF have different structures, which have different number of atoms such as carbon and oxygen. For the estimated values of  $T_c$  and  $P_c$  from the JOBACK method, the differences are more noticeable for HMF-levulinate and HMF-lactate, likely due to the different number of the groups (such as -CH<sub>2</sub>, O-H, ring group, non-ring group, and -O-), which significantly affect the contributions of these groups. The results obtained from this study confirm that the thermodynamic property values of the molecules is strong dependent on the actual structure of the molecule and the specific contribution of the particular group. The GANI method was employed to estimate the value of  $\Delta G_f^0(298.15)$  and  $(\Delta_f H_{298.15}^0(g))$  for HMF-esters. The negative value of

Table 2 Comparison of the esterification reactions with the present study<sup>a</sup>

Reactants	Catalysts	Activation energy (kJ mol <sup>-1</sup> )	References
<i>n</i> -Butanol and LA	Sulfuric acid	54.27	74
Isobutyl alcohol and palmitic acid	Sulfuric acid	58.0	75
Palmitic acid and isopropanol	<i>p</i> -TSA	40.77	76
Palmitic acid and isobutyl alcohol	Composite catalytic membrane (CCM)	35.97	77
Benzyl alcohol and acetic acid	Dowex 50 Wx8-catalyst	54.5–57	69
Ethanol and acrylic acid	Amberlyst 35	59.60	68
Methanol and oleic acid	UiO-66 MOF	54.9 ± 1.8	70
5-HMF and LA	Novozym 435	NR	27
5-HMF and LA	[SMIM][FeCl <sub>4</sub> ]	32.78	This study

<sup>a</sup> NR = Not reported.

Table 3 Estimated thermodynamic properties of the HMF-ester compounds using group contribution methods

Methods	Properties	HMF-levulinate	HMF-lectate	HMF-propionate	HMF-Acetate	HMF-formate
JOBACK	$T_c(K)$	777	799	745	745	744
	$P_c(\text{bar})$	28.11	33.1	32.4	30.6	43.2
GANI	$T_b(K)$	593.15	601.05	546.10	539.24	630.62
	$\Delta H_f^0(\text{J mol}^{-1})$	-681 × 10 <sup>3</sup>	-664 × 10 <sup>3</sup>	-541 × 10 <sup>3</sup>	-471 × 10 <sup>3</sup>	-459 × 10 <sup>3</sup>
	$\Delta G_f^0(\text{J mol}^{-1})$	-446 × 10 <sup>3</sup>	-459 × 10 <sup>3</sup>	-459 × 10 <sup>3</sup>	-341 × 10 <sup>3</sup>	-332 × 10 <sup>3</sup>
LYDERSEN	$V_c(\text{m}^3 \text{kmol}^{-1})$	0.627	0.568	0.512	0.423	0.401



Table 4 Estimated value of ideal gas heat capacity  $C_p$  (J mol<sup>-1</sup> K<sup>-1</sup>) for HMF-ester products at constant pressure using the BENSON method

Ester products	373 (K)	473 (K)	573 (K)	673 (K)	773 (K)	873 (K)	973 (K)	1073 (K)	1173 (K)	1273 (K)
HMF-levulinate	299.8	348.4	390.6	428.8	457.0	481.7	500.8	514.7	523.4	527.3
HMF-formate	187.0	216.9	243.4	266.4	285.5	300.5	311.3	317.7	319.4	326.2
HMF-lactate	262.3	304.1	341.1	373.2	400.3	422.3	439.1	450.7	456.8	457.6
HMF-propionate	243.8	284.4	319.7	350.0	375.4	395.8	411.5	422.6	426.2	431.4
HMF-acetate	215.0	250.2	281.4	308.0	330.3	348.0	365.3	369.2	372.4	379.0

( $\Delta_f H_{298.15}^0$ (g)) and  $\Delta G_f^0(298.15)$  for (HMF-levulinate, HMF-acetate, HMF-propionate, HMF-lactate, and HMF-formate) compounds indicates that the product formation from each reaction step can proceed spontaneously. In this comparison, similarly, enthalpy and Gibbs free energy of formation of HMF-ester compounds at 298 K were also calculated using the GANI method, and the values are shown in Table 3.

Following the JOBACK and BENSON GCMs, the estimated value for the idea gas heat capacity for 5-HMF in the temperature range from 273 K to 1273 K is shown in Table 4 and compared in Tables S2 and S3 (ESI).<sup>†</sup> The estimated physical properties were compared and the percentage error was calculated. Finally, the compared results confirm that the BENSON method fitted well with the experimental findings with minimum percentage error and gave more accurate results, whereas the JOBACK method shows relatively low accuracy. Table 4 shows the predicted values of ideal gas heat capacities in the temperature range from 273 K to 1273 K for HMF-ester products using the BENSON method.

## 4. Conclusion

In this study, the laboratory synthesis of the bifunctional IL catalyst [SMIM][FeCl<sub>4</sub>] was done and characterized using <sup>1</sup>H and <sup>13</sup>C NMR spectroscopic techniques. The catalytic activity of the laboratory-synthesized bifunctional IL catalyst [SMIM][FeCl<sub>4</sub>] was investigated for the esterification of 5-HMF with LA to HMF-levulinate. The effect of the reaction time and temperature on the 5-HMF conversion to HMF-levulinate was investigated. Further, the kinetic modelling of this esterification reaction was carried out. To determine the reaction kinetic parameters, the effects of the reaction conditions such as reaction time and temperature on 5-HMF conversion were investigated. A maximum (97%) 5-HMF conversion and 78% yield of HMF-levulinate were achieved at 378.15 K in 5 h. The kinetics of the HMF-levulinate synthesis were investigated in a batch reactor. The activation energy  $E_a$  for this reaction was 32.78 kJ mol<sup>-1</sup> for first order kinetics. The thermodynamic properties such as  $T_c$ ,  $V_c$ ,  $P_c$ ,  $\Delta G_f^0$ ,  $\Delta_f H^0$ , and  $C_p$  for the HMF-ester products (HMF-acetate, HMF-formate, HMF-levulinate, HMF-propionate, and HMF-lactate), which are not reported in the literature so far, were estimated using the GCMs. Overall, these new insights into the reaction thermodynamics and kinetics of the esterification of 5-HMF with biomass-derived acids will be extremely useful for the development of a green process route for the valorization of waste biomass into potentially useful ester products.

## Conflicts of interest

There are no conflicts to declare.

## Acknowledgements

Komal Kumar thanks University Grants Commission (UGC), India, for a research fellowship. Dr Sreedevi Upadhyayula is thankful to Ministry of Human Resource Development (MHRD), Government of India for financial grant no. SPARC/P1318. The authors are also thankful to NRF (Nanoscale Research Facility) for providing High pressure liquid chromatography (HPLC) for the detection of 5-HMF conversion at IIT Delhi. One of the authors Dr Anthony Halog gratefully acknowledges funding support from the University of Queensland, Australia under the UQ Global Strategy and Partnerships Seed Funding Scheme: Round Two 2022.

## References

- V. S. Sikarwar, M. Zhao, P. Clough, J. Yao, X. Zhong, M. Z. Memon, N. Shah, E. J. Anthony and P. S. Fennell, *Energy Environ. Sci.*, 2016, **9**, 2939–2977.
- X. Zhao, H. Zhou, V. S. Sikarwar, M. Zhao, A. H. A. Park, P. S. Fennell, L. Shen and L. S. Fan, *Energy Environ. Sci.*, 2017, **10**, 1885–1910.
- A. Saravanan, S. Jeevanantham, P. Senthil Kumar, S. Varjani, P. R. Yaashikaa and S. Karishma, *Ind. Crops Prod.*, 2020, **153**, 112613.
- S. Takkellapati, T. Li and M. A. Gonzalez, *Clean Technol. Environ. Policy*, 2018, **20**, 1615–1630.
- M. J. Climent, A. Corma and S. Iborra, *Green Chem.*, 2014, **16**, 516–547.
- S. Jing, X. Cao, L. Zhong, X. Peng, R. Sun and J. Liu, *Ind. Crops Prod.*, 2018, **126**, 151–157.
- E. C. Nnadozie and P. A. Ajibade, *Chem. Data Collect.*, 2021, **33**, 100673.
- S. Pathak, A. K. Ray, H. Großmann and R. Kleinert, *Radiat. Phys. Chem.*, 2015, **117**, 59–63.
- F. M. Fadul, *Acta Innov.*, 2019, 47–56.
- M. Stöcker, *Angew. Chem., Int. Ed.*, 2008, **47**, 9200–9211.
- S. Kang, J. Fu and G. Zhang, *Renewable Sustainable Energy Rev.*, 2018, **94**, 340–362.
- A. M. Da Costa Lopes, R. M. G. Lins, R. A. Rebelo and R. M. Łukasik, *Green Chem.*, 2018, **20**, 4043–4057.
- L. Zhou, R. Liang, Z. Ma, T. Wu and Y. Wu, *Bioresour. Technol.*, 2013, **129**, 450–455.



- 14 A. M. Borrero-López, E. Masson, A. Celzard and V. Fierro, *Ind. Crops Prod.*, 2018, **124**, 919–930.
- 15 I. Delidovich, K. Leonhard and R. Palkovits, *Energy Environ. Sci.*, 2014, **7**, 2803–2830.
- 16 K. Kumar, F. Parveen, T. Patra and S. Upadhyayula, *New J. Chem.*, 2018, **42**, 228–236.
- 17 M. E. Zakrzewska, E. Bogel-Lukasik and R. Bogel-Lukasik, *Chem. Rev.*, 2011, **42**, 397–417.
- 18 A. A. Rosatella, S. P. Simeonov, R. F. M. Frade and C. A. M. Afonso, *Green Chem.*, 2011, **13**, 754–793.
- 19 Y. S. Qu, Y. L. Song, C. P. Huang, J. Zhang and B. H. Chen, *Ind. Eng. Chem. Res.*, 2012, **51**, 13008–13013.
- 20 D. J. Braden, C. A. Henao, J. Heltzel, C. C. Maravelias and J. A. Dumesic, *Green Chem.*, 2011, **13**, 1755–1765.
- 21 F. A. Kucherov, L. V. Romashov, K. I. Galkin and V. P. Ananikov, *ACS Sustainable Chem. Eng.*, 2018, **6**, 8064–8092.
- 22 M. Li, G. Li, N. Li, A. Wang, W. Dong, X. Wang and Y. Cong, *Chem. Commun.*, 2014, **50**, 1414–1416.
- 23 K. Kumar, A. Dahiya, T. Patra and S. Upadhyayula, *ChemistrySelect*, 2018, **3**, 6242–6248.
- 24 K. Kumar, S. Pathak and S. Upadhyayula, *J. Cleaner Prod.*, 2020, **256**, 120292.
- 25 Z. Zhang, J. Zhen, B. Liu, K. Lv and K. Deng, *Green Chem.*, 2015, **17**, 1308–1317.
- 26 Y. Zhu, X. Kong, H. Zheng, G. Ding, Y. Zhu and Y. W. Li, *Catal. Sci. Technol.*, 2015, **5**, 4208–4217.
- 27 Y. Z. Qin, M. H. Zong, W. Y. Lou and N. Li, *ACS Sustainable Chem. Eng.*, 2016, **4**, 4050–4054.
- 28 M. Krystof, M. Pérez-Sánchez and P. Domínguez De María, *ChemSusChem*, 2013, **6**, 630–634.
- 29 V. K. Mishra, F. Temelli and B. Ooraikul, *J. Food Eng.*, 1994, **23**, 467–480.
- 30 N. Bureau, J. Jose, I. Mokbel and J. C. De Hemptinne, *J. Chem. Thermodyn.*, 2001, **33**, 1485–1498.
- 31 M. Moosavi, *Fluid Phase Equilib.*, 2012, **316**, 122–131.
- 32 X. Han and L. Zhou, *Chem. Eng. J.*, 2011, **172**, 459–466.
- 33 D. Zhao, M. Liu, J. Zhang, J. Li and P. Ren, *Chem. Eng. J.*, 2013, **221**, 99–104.
- 34 T. Joseph, S. Sahoo and S. B. Halligudi, *J. Mol. Catal. A: Chem.*, 2005, **234**, 107–110.
- 35 J. Gui, X. Cong, D. Liu, X. Zhang, Z. Hu and Z. Sun, *Catal. Commun.*, 2004, **5**, 473–477.
- 36 J. Keogh, M. S. Tiwari and H. Manyar, *Ind. Eng. Chem. Res.*, 2019, **58**, 17235–17243.
- 37 J. P. Hallett and T. Welton, *Chem. Rev.*, 2011, **111**, 3508–3576.
- 38 D. Yujaroen, M. Goto, M. Sasaki and A. Shotipruk, *Fuel*, 2009, **88**, 2011–2016.
- 39 W. Sakdasri, R. Sawangkeaw and S. Ngamprasertsith, *Asia-Pac. J. Chem. Eng.*, 2016, **11**, 539–548.
- 40 N. S. Evangelista, F. R. Do Carmo and H. B. De Sant'Ana, *Ind. Eng. Chem. Res.*, 2017, **56**, 2298–2309.
- 41 N. S. Evangelista, F. R. Do Carmo and H. B. De Sant'Ana, *Ind. Eng. Chem. Res.*, 2018, **57**, 8552–8565.
- 42 S. V. D. Freitas, M. B. Oliveira, Á. S. Lima and J. A. P. Coutinho, *Energy Fuels*, 2012, **26**, 3048–3053.
- 43 W. Cordes and J. Rarey, *Fluid Phase Equilib.*, 2002, **201**, 409–433.
- 44 P. Saxena, J. Patel and M. H. Joshipura, *Fuel*, 2016, **182**, 842–849.
- 45 O. C. Díaz, F. Schoeggl, H. W. Yarranton, M. A. Satyro, T. M. Lovestead and T. J. Bruno, *Int. J. Chem., Mol., Nucl., Mater. Metall. Eng.*, 2012, **6**, 460–470.
- 46 W. Su, L. Zhao and S. Deng, *Renewable Sustainable Energy Rev.*, 2017, **79**, 984–1001.
- 47 D. H. Zaitsau, A. A. Pimerzin and S. P. Verevkin, *J. Chem. Thermodyn.*, 2019, **132**, 322–340.
- 48 W. Yuan, A. C. Hansen and Q. Zhang, *Fuel*, 2005, **84**, 943–950.
- 49 L. Constantinou and R. Gani, *AIChE J.*, 1994, **40**, 1697–1710.
- 50 J. Marrero and R. Gani, *Fluid Phase Equilib.*, 2001, **183–184**, 183–208.
- 51 Z. Kolská, V. Růžička and R. Gani, *Ind. Eng. Chem. Res.*, 2005, **44**, 8436–8454.
- 52 A. M. Benkouider, R. Kessas, S. Guella, A. Yahiaoui and F. Bagui, *J. Mol. Liq.*, 2014, **194**, 48–56.
- 53 I. Cachadiña and A. Mulero, *Fluid Phase Equilib.*, 2009, **287**, 33–38.
- 54 W. L. Kubic, R. W. Jenkins, C. M. Moore, T. A. Semelsberger and A. D. Sutton, *Ind. Eng. Chem. Res.*, 2017, **56**, 12236–12245.
- 55 H. Grensemann and J. rgen Gmehling, *Ind. Eng. Chem. Res.*, 2005, **44**, 1610–1624.
- 56 K. G. Joback and R. C. Reid, *Chem. Eng. Commun.*, 1987, **57**, 233–243.
- 57 J. Marrero-Morejón and E. Pardillo-Fontdevila, *AIChE J.*, 1999, **45**, 615–621.
- 58 X. Wen and Y. Qiang, *Ind. Eng. Chem. Res.*, 2001, **40**, 6245–6250.
- 59 J. Li, L. Xia and S. Xiang, *Fluid Phase Equilib.*, 2016, **417**, 1–6.
- 60 Y. Yoneda, *Bull. Chem. Soc. Jpn.*, 1979, **52**, 1297–1314.
- 61 R. Ceriani, R. Gani and Y. A. Liu, *Fluid Phase Equilib.*, 2013, **337**, 53–59.
- 62 B. Moller, J. Rarey and D. Ramjugernath, *J. Mol. Liq.*, 2008, **143**, 52–63.
- 63 M. Sales-Cruz, G. Aca-Aca, O. Sánchez-Daza and T. López-Arenas, *20th Eur. Symp. Comput. Aided Process Eng. ESCAPE20*, 2010, pp. 1–6.
- 64 T. Wallek, K. Knöbelreiter and J. Rarey, *Ind. Eng. Chem. Res.*, 2018, **57**, 3382–3396.
- 65 T. Y. Wang, X. Z. Meng, M. Jia and X. C. Song, *Fuel Process. Technol.*, 2015, **131**, 223–229.
- 66 J. F. Pankow and W. E. Asher, *Atmos. Chem. Phys.*, 2008, **8**, 2773–2796.
- 67 M. M. Zainol, N. A. S. Amin and M. Asmadi, *Renewable Energy*, 2019, **130**, 547–557.
- 68 J. W. Lin, A. H. Zaki, H. T. Wu, H. mu Lin and M. J. Lee, *J. Taiwan Inst. Chem. Eng.*, 2019, **102**, 44–50.
- 69 S. H. Ali and S. Q. Merchant, *Ind. Eng. Chem. Res.*, 2009, **48**, 2519–2532.
- 70 S. Chaemchuen, P. M. Heynderickx and F. Verpoort, *Chem. Eng. J.*, 2020, **394**, 124816.



- 71 N. A. S. Ramli and N. A. S. Amin, *J. Mol. Catal. A: Chem.*, 2015, **407**, 113–121.
- 72 K. Kumar, V. Khatri, F. Parveen, H. K. Kashyap and S. Upadhyayula, *Sustainable Energy Fuels*, 2020, **4**, 2924–2936.
- 73 F. R. Carmo, N. S. Evangelista, F. A. N. Fernandes and H. B. D. S. Ana, *J. Chem. Eng. Data*, 2015, **60**, 3358–3381.
- 74 H. J. Bart, J. Reidetschläger, K. Schatka and A. Lehmann, *Int. J. Chem. Kinet.*, 1994, **26**, 1013–1021.
- 75 S. Goto, T. Tagawa and A. Yusoff, *Int. J. Chem. Kinet.*, 1991, **23**, 17–26.
- 76 R. Aafaqi, A. R. Mohamed and S. Bhatia, *J. Chem. Technol. Biotechnol.*, 2004, **79**, 1127–1134.
- 77 W. Shi, B. He, Y. Cao, J. Li, F. Yan, Z. Cui, Z. Zou, S. Guo and X. Qian, *Bioresour. Technol.*, 2013, **129**, 100–107.
- 78 M. Krystof, M. Pérez-Sánchez and P. Domínguez De María, *ChemSusChem*, 2013, **6**, 630–634.

